Int. J. Electrochem. Sci., 8 **(2013)** 5605 - 5612

International Journal of
ELECTROCHEMICAL
SCIENCE
www.electrochemsci.org

Synergistic Effect of 2-Amino-5-(Ethylthio)-1,3,4-Thiadiazole and Chloride Ion on Cu Anodic Dissolution in a Phosphate-Based Electrolyte

Shu-Wei Chou, Hsiao-Ching Chang and Jeng-Yu Lin[*]

Department of Chemical Engineering, Tatung University, No. 40, Sec. 3, ChungShan North Rd., Taipei City 104, Taiwan
[*]E-mail: jylin@ttu.edu.tw

Received: 6 February 2013 / *Accepted:* 11 March 2013 / *Published:* 1 April 2013

In this work, the synergistic effect of 2-amino-5-(ethylthio)-1,3,4-thiadiazole (AETD) and chloride ion (Cl^-) in a phosphate-based electrolyte was systemically studied. The results from X-ray photoelectron spectrometer indicate that Cl^- was indeed incorporated into the AETD-containing passive film. According to extensive electrochemical and material analyses, the inhibition capability of the Cl^--incorporated AETD passive film demonstrated superior corrosion resistance for Cu anodic dissolution compared the AETD passive film alone due to the formation of dense passive film. Additionally, the combined of AETD and Cl^- in the phosphate-based electrolyte had a wide potential window within the planarization efficiency and the Cu removal rate were great than 70% and 600 nm min^{-1}, respectively, thus demonstrating its great potential as an electrolyte for electrochemical mechanical planarization.

Keywords: ??

1. INTRODUCTION

Cu metal has been widely used in microelectronic industry due to its lower resistance and higher reliability compared to Al metal [1,2]. Nevertheless, Cu is an active metal and thus the oxidation of Cu is considered a critical reliability problem during microelectronic fabrication processing. Azole-containing compounds are usually used as corrosion inhibitors, in which protonated nitrogen atoms can coordinate with Cu(0), Cu(I) or Cu(II) by forming Cu-azole complex against Cu corrosion [3-10]. Among them, the corrosion inhibitor, 2-amino-5-(ethylthio)-1,3,4-thiadiazole (AETD), has demonstrated its excellent corrosion resistance. Sherif et al. [11] found that AETD possessed high inhibition efficiency for Cu corrosion due to its specific molecular structure containing

a variety of donor atoms. Sherif et al. [12] further demonstrated the inhibition efficiency in 3% NaCl aqueous solution can achieved about 94% in the presence of AETD.

In this study, we first tried to employ AETD as a corrosion inhibitor for Cu anodic dissolution in a phosphate-based electrolyte. Additionally, the influence of chloride ion on the corrosion resistance of AETD was investigated. Eventually, we employed the synergistic result of AETD and chloride ion (Cl^-) in the phosphate-based electrolyte for Cu electrochemical mechanical planarization (ECMP), in which an accelerated electrochemical Cu removal can be obtained from the surface elevations because the original passive films formed from the inhibitors are abraded away, coupled with little or no removal at surface recesses, where the passive films remain intact [13]. After polishing in a simulated device, a high planarization efficiency can be achieved when using the phosphate-based electrolyte both containing AETD and Cl^-.

2. EXPERIMENTAL

2.1 Preparation of electrolyte

The phosphate-based electrolyte was prepared with de-ionized water and 1 M potassium phosphate (monobasic, Sigma-Aldrich), containing modicums of ortho-phosphoric acid (Merk, 85%) at pH 2. Analytical grade chemical, 2-amino-5-(ethylthio)-1,3,4-thiadiazole AETD and potassium chloride (KCl) were purchased from Sigma–Aldrich and Fisher Scientific as a corrosion inhibitor and Cl^- source, respectively.

2.2. Electrochemical measurements

The potentiodynamic polarization and impedance measurements were both carried out by using CHI 614D (CH Instrument) potentiostat in a three-electrode cell. During potentiodynamic polarization measurements and electrochemical polishing experiments, a Cu rotating disk electrode (RDE, 0.5 cm^2) and a 99.99% Cu foil (1 cm^2) were mounted onto a rotator adaptor as working electrodes, respectively. The rotation speed of 100 rpm was employed for the aforementioned measurements. In addition, a Pt wire and a saturated sliver/sliver chloride (Ag/AgCl) were used as a counter electrode and a reference electrode, respectively. For potentiodynamic experiments, potential interval was swept from 0 to 2.5V vs. Ag/AgCl at a scan rate of 5mV s^{-1}.

2.3. Characterization of passive films

Prior to the characterization of passive films formed from the inhibitor, Cu foils were electropolsing in ortho-phosphoric acid at constant potential of 1.2V vs. Ag/AgCl for 1 h. The surface morphology was characterized by an atomic force microscope (AFM, NS3a controller with D3100 stage; Digital Instruments) in tapping mode at a scan rate of 0.8 Hz. The composition of the passive film was studied using an x-ray photoelectron spectrometer (XPS, ULVAC-PHI, PHI Quantera SXM).

2.4. Polishing experiments

The Cu ECMP was executed in a specially designed polishing cell. During the potentiodynamic measurements with and without abrasion, the Cu foil (1cm^2) was rotated at 100 rpm on a polishing pad (Buehler) under a pressure of ~0.5 psi.

3. RESULTS AND DISCUSSION

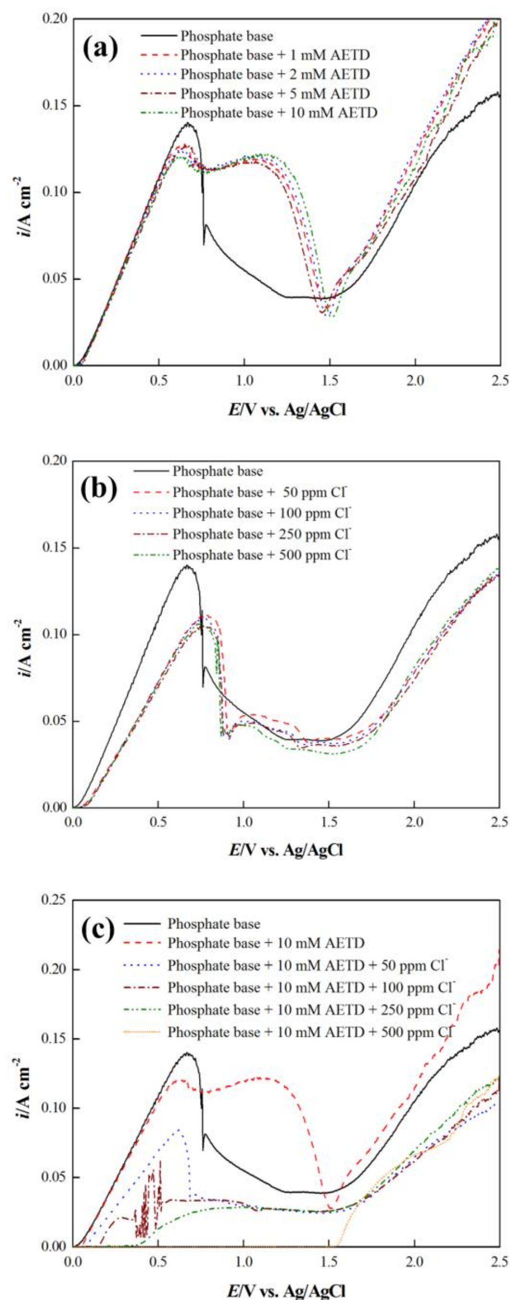

Figure 1. Potentiodynamic polarization curves at scan rate of 5 mV^{-1} measured Cu RDE with a rotation speeds of 100 rpm in solutions: (a) AETD-containing phosphate-based electrolyte; (b) Cl^--containing phosphate-based electrolyte; (c) phosphate-base electrolyte both containing of AETD and Cl^-.

According to the previous study, Shattuck et al. [14] revealed that the RDE experiment is an efficient method to evaluate the electrolyte properties and inhibition efficiency of inhibitors. Potentiodynamic polarization measurements were carried out using RDE adapter to study the effect of AETD, Cl^- and both containing in the phosphate electrolyte are shown in Fig. 1. Fig. 1a shows the effect of various concentration of AETD introducing in phosphate electrolyte. Obviously, there is no significant decrease in the current density when adding the AETD inhibitor into the phosphate-based electrolyte with the concentrations from 0.001M to 0.01M. This result indicates that a phosphate-based electrolyte containing AETD alone cannot suffer from the Cu dissolution. Fig. 1b shows the polarization curves obtained in phosphate-based electrolyte with Cl^- concentrations from 0 to 500 ppm. When the concentration of Cl^- increased, the current density only slightly decreased, which possibly resulted in formation Cl^--containing film on Cu surface. This result indicated that Cl^- introducing in phosphate-based electrolyte was also ineffective against Cu anodic dissolution. However, the current density decreased significantly (as shown in Fig. 1c) when Cl^- was introduced into the phosphate-based electrolyte containing AETD. This suggests that the inhibition capability of AETD was enhanced due to the introduction of Cl^- into AETD-containing phosphate-based electrolyte. In addition, the inhibition region was expended from 0 to ~1.5 V vs. Ag/AgCl after 500 ppm Cl^- introduced into AETD-containing phosphate-based electrolyte. Therefore, the addition of Cl^- can facilitate enhancing the inhibition capability of AETD passive film, even at high anodic potential.

In order to clarify the enhancement in inhibition capability of AETD passive film when introducing Cl^- into the phosphate-based electrolyte contining AETD, the XPS studies were carried out to characterize the chemical composition of the passive films formed on Cu substrates in the AETD-contining phosphate-based electrolyte with and without Cl^-.

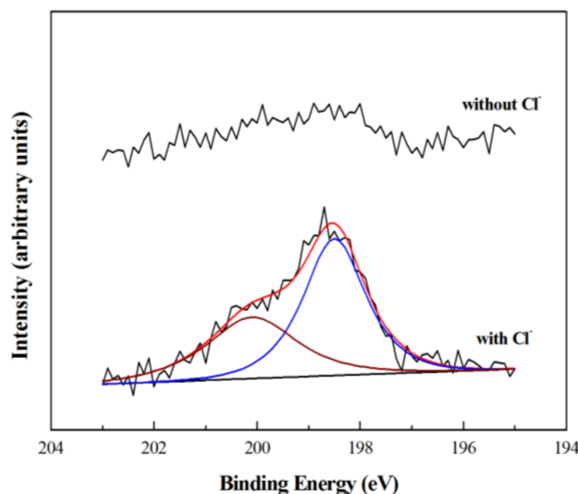

Figure 2. Cl 2p XPS spectra of the electropolished Cu foils immersed in the AETD-containing phosphate-based electrolyte without and with 500 ppm Cl^-.

Fig. 2 shows Cl 2p XPS spectra of the electropolished Cu foils immersed in the AETD-containing phosphate-based electrolyte without and with 500 ppm Cl^- at a constant applied potential of

0.3 V vs. Ag/AgCl for 180 s. Apparently, there is no peak detected in Cl $2p_{3/2}$ XPS spectra when the phosphate-based electolyte only contains 0.01M AETD. However, the Cl $2p_{3/2}$ peak can be observed after 500 ppm Cl^- is introduced into the AETD-containing phosphate-based electrolyte. Therefore, the XPS measurements reveal that the enhancement of inhibition capability can be attributed to the incorporation of Cl^- into the AETD passive film.To further characterize the surface evolution when introducing Cl^- into the phosphate-based electrolyte, the AFM analyses were conducted to characterize the surface morphology of Cu before and after the chronoamperometric treatments. Fig. 3a shows the smooth morphology of the Cu foil obtained after electropolishing in phosphoric acid for 1 hr, in which the surface average roughness was only approximately 1 nm. Fig. 3b-e shows the AFM 2D images obtained from the electropolished Cu foils after the chronoamperometric measurements in various electrolytes at 0.3 V vs. Ag/AgCl for 180 s. According to Fig. 3b and 3c, the Cu surface morphology of phosphate-based electrolyte containing without and with AETD were similar and the surface roughness were about 67 and 66 nm, respectively. This indicates that the addition of AETD alone in the phosphate-based electrolyte was unable to against Cu anodic dissolution. As for the case of the phosphate-based electrolyte containing 500 ppm Cl^-, its surface roughness was increased from 67 to 82nm because there were many large particles formed on Cu surface (Fig. 3d), which can be attributed to the formation of Cu-chloride complexes on Cu surface. Fig. 3e presents the Cu surface morphology after treating in the phosphate-based electrolyte both containing AETD and Cl^-. It can be noted that a dense passive film composed of lots of small particles formed on the Cu foil. This implies that the phosphate-based electrolyte both containing AETD and Cl^- can be against Cu anodic dissolution due to the formation of dense Cl^--containing AETD passive film on the Cu foil.

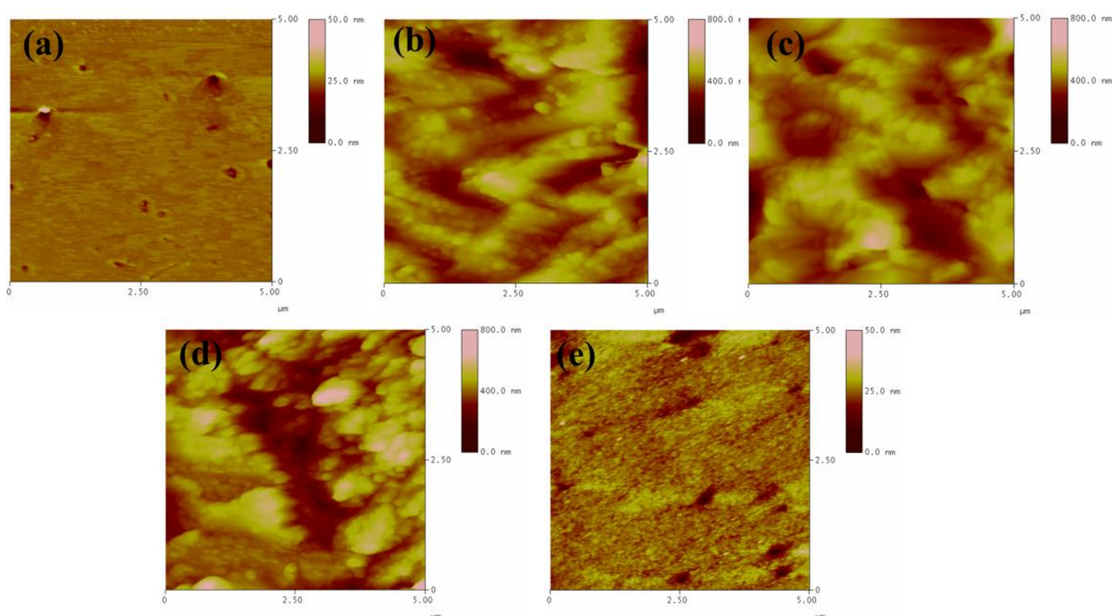

Figure 3. AFM images Cu foils after following treatments: (a) electropolishing alone. After electropolishing, the Cu foils were immersed in the following solutions at a constant potential of 0.3 V vs. Ag/AgCl for 180 s: (b) phosphate-based electrolytes; (c) phosphate-based electrolyte containing 0.01 M AETD; (d) phosphate-based electrolyte containing 500 ppm Cl^-; (e) phosphate-based electrolyte containing 0.01 M AETD + 500 ppm Cl^-.

Based on the aforementioned results, the phosphate-based electrolyte both containing AETD and Cl^- exhibits great potential against Cu anodic dissolution. Herein, the electrolyte was further evaluated for ECMP process by using a specially designed acrylic polishing device. To demonstrate if the electrolyte can be used for ECMP, the potentiodynamic curves of Cu foils with and without abrasion in phosphate-based electrolytes containing 0.01M AETD and 500 ppm Cl^- were performed and shown in Fig. 4. The effective operating potential window for AETD passive film was achieved to ~1.5 V vs. Ag/AgCl forming in the phosphate-based electrolyte containing 0.01M AETD and 500 ppm Cl^-. It can be noted that the current densities increased for both case when Cu foils contacted with polishing pad. These results indicate that the increase in current density may be mainly due to the removal of passive film. Here, the current oscillations generally occur due to the instantaneous Cu dissolution or the regeneration of surface oxide films [15,16]. In addition, the Cu remove were mainly relies on the applied external current, therefore the Cu removal rate can be estimated through Faraday's law. The results of Cu planarization factor, ε_{ECMP}, can be defined as follows [6,14,17]:

$$\varepsilon_{ECMP} = \frac{i_{abrasion} - i_{noabrasion}}{i_{abrasion}} \quad (1)$$

Figure 5 shows the ε_{ECMP} and Cu removal rate in ECMP process which were estimated by Eq. (1) and the potentiodynamic curves shown in Fig.4. The results show the incorporation of Cl^- in AETD passive film, an effective protection of Cu against dissolution can be demonstrated at high anodic potentials (~1.5 V vs. Ag/AgCl) in which ε_{ECMP} can achieve above 0.95. Tripathi et al. [6] indicated a good ECMP electrolytes have possess of the removal rates higher than 600nm min^{-1}.

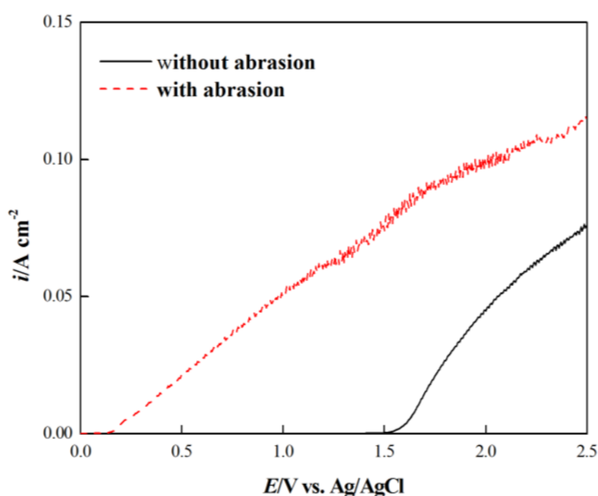

Figure 4. Potentiodynamic polarization curves at scan rate of 5mV^{-1} measured without and with abrasion in the phosphate-based electrolyte containing 0.01 M AETD + 500 ppm Cl^-. Rotation speeds of 100 rpm were used during the measurements.

Consequently, consider the removal rates during ECMP process in the phosphate based electrolyte both containing 0.01 M AETD and 500 ppm Cl^- is useful when the external potential higher

than 0.7 V vs. Ag/AgCl. Considering the electrolyte containing 0.01 M AETD and 500 ppm Cl^- of ε_{ECMP} and removal rate, the suitable operate potential window from 0.7 V to 1.5 V vs. Ag/AgCl which obtained the Cu removal rate is higher than 600 nm/min and the ε_{ECMP} is higher than 0.95.

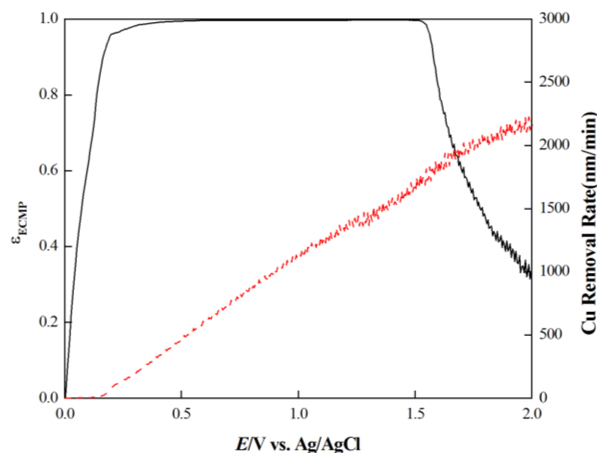

Figure 5. Calculated planarization factor (—) and Cu removal rate (- -) for the phosphate-based electrolyte containing 0.01 M AETD + 500 ppm Cl^-.

4. CONCLUSIONS

In summary, a phosphate-based electrolyte containing both AETD and Cl^- showed an enhanced performance against Cu anodic dissolution by the incorporation of Cl^- into AETD passive film. The incorporation of Cl^- made the AETD passive film sufficiently and densely adsorbed onto the Cu foil, thus resulting in the enhancement in the corrosion resistance for Cu anodic dissolution. When the phosphate-based electrolyte containing AETD and Cl^- was tested in a simulated ECMP process, a high planarization efficiency can be obtained. Therefore, the phosphate-based electrolyte containing AETD and Cl^- showed a promising potential for use in ECMP process.

ACKNOWLEDGEMENTS
This research was supported by National Science Council Taiwan (NSC 101-2221-E-036-035) and Tatung University (B98-C11-010).

References

1. S.P. Murarka, *Mater. Sci. Eng. R.*, 19 (1997) 87.
2. R. Rosenberg, D.C. Edelstein, C.K. Hu, K.P. Rodbell, *Ann. Rev. Mater. Sci.*, 30 (2000) 229.
3. V. Lakshminarayanan, R. Kannan, S.R. Rajagopalan, *J. Electroanal. Chem.,* 364 (1994) 79.
4. A. Jindal, S. V. Babu, *J. Electrochem. Soc.*, 151 (2004) G709.
5. J.W. Lee, M.C Kang, J.J Kim, *J. Electrochem. Soc.*, 152 (2005) C827.
6. A. Tripathi, C. Burkhard, I.I. Suni, Y. Li, F. Doniat, A. Barajas, J. McAndrew, *J. Electrochem. Soc.,* 155 (2008) H918.

7. D. Chadwick, T. Hashemi, *Surf. Sci.* 89 (1979) 649.
8. W.J. Lee, *Mater. Sci. Eng. A*, 348 (2003) 217.
9. J.Y. Lin, S.W. Chou, *Electrochim. Acta,* 56 (2011) 3303.
10. J.Y. Lin, S.W. Chou, *Int. J. Electrochem. Sci.,* 7 (2012) 3527.
11. E.M. Sherif, S.M. Park, *Corros. Sci.,* 48 (2006) 4065.
12. E.M. Sherif, *J. Appl. Surf. Sci.,* 252 (2006) 8615.
13. F.Q. Liu, T. Du, A. Duboust, S. Tsai, W.Y. Hsu, *J. Electrochem. Soc.,* 153 (2006) C377.
14. K.G. Shattuck, J.Y. Lin, P. Cojocaru, A.C. West, *Electrochim. Acta,* 53 (2008) 8211.
15. V.A. Dmitriev, E.V. Rzhevskaya, *Russ. J. Phys. Chem.,* 35 (1961) 425.
16. B. Pointu, *Electrochim. Acta*, 14 (1969) 1207.
17. D. Padhi, J. Yahalom, S. Gandikota, G. Dixit, *J. Electrochem. Soc.,* 150 (2003) G10.

© 2013 by ESG (www.electrochemsci.org)